

# Rates of $D_0^*(2400)$ , $D_J^*(3000)$ as the $D_0^*(2P)$ and $D_0^*(3P)$ in $B$ Decays

Xiao-Ze Tan, Yue Jiang<sup>a</sup>, Tianhong Wang, Tian Zhou, Geng Li, Zi-Kan Geng, Guo-Li Wang

*Department of Physics, Harbin Institute of Technology,*

*Harbin, 150001, People's Republic of China*

## Abstract

In this paper, we use the instantaneous Bethe-Salpeter method to calculate the semi-leptonic and non-leptonic production of the orbitally excited scalar  $D_0^*$  in  $B$  meson decays. When the final state is  $1P$  state  $D_0^*(2400)$ , our theoretical decay rate is consistent with experimental data. For  $D_J^*(3000)$  final state, which was observed by LHCb collaboration recently and here treated as the orbitally excited scalar  $D_0^*(2P)$ , its rate is in the order of  $10^{-4} \sim 10^{-6}$ . We find the special node structure of  $D_0^*(2P)$  wave function possibly results in the suppression of its branching ratio and the abnormal uncertainty. The  $3P$  states production rate is in the order of  $10^{-5}$ .

**Keywords:** Orbitally excited scalar,  $D$  mesons; Semi-leptonic; Non-leptonic; Bethe-Salpeter Method.

---

<sup>a</sup> jiangure@hit.edu.cn

## I. INTRODUCTION

The semi-leptonic and non-leptonic decays of  $B$  mesons are the frequently studied decays and also the dominant production channels of charmed mesons. During the last decades, for many important cases such as providing precise value of CKM element  $V_{cb}$ , the channels of  $B$  decays to S-wave ground states of  $D$  mesons have been extensively measured and studied by the ALEPH, CLEO, OPAL, BABAR and Belle Collaborations[1–8] besides the theoretical studies.

In recent years, many collaborations reported several charmed resonances including some orbitally excited  $D$  mesons, which attracts lots of attention. The Belle and BABAR Collaborations reported the semi-leptonic  $B$  decays to P-wave  $D^*$  mesons by using fully reconstructed  $B$  tags [9, 10] and the Belle, BABAR and LHCb Collaborations reported the non-leptonic decays  $B \rightarrow D_0^* \pi(K)$  [11–15]. They inspired many theoretical studies on the excited charmed states using different models, for example, the light-front quark model [16], the constituent quark model[17], as well as the Bethe-Salpeter method [18], etc.

In 2013, the LHCb Collaboration reported several resonances around 3000 MeV,  $D_J(3000)^0$  and  $D_J^*(3000)^{+,0}$ [19]. The  $D_J(3000)$  and  $D_J^*(3000)$  were observed in the  $D^* \pi$  and  $D \pi$  invariant mass spectrum respectively. Their quantum numbers  $J^P$  are still undetermined and many theoretical studies give different assignments [20–23]. In our previous works[24, 25], we calculated the strong decays and the leptonic productions of  $D_J(3000)$  and we favoured it as the excited  $2P(1^{+'})$  broad state. For  $D_J^*(3000)$ , we calculated its strong decays and our results favoured it as the excited scalar  $2P(0^+)$  state [26].

We notice that, in current experiments and theories, the knowledge of  $B$  semi-leptonic and non-leptonic decays to orbitally excited  $D_0^*$  meson is still rather poor. Thus this work will focus on the leptonic decays  $B \rightarrow D_0^* \ell^- \bar{\nu}_\ell$  and non-leptonic decays  $B \rightarrow D_0^* X$ , where the initial state could be  $B^-$  or  $\bar{B}^0$ , the final state  $D_0^*$  is the excited scalar  $D_0^*(nP)^0$  or  $D_0^*(nP)^+$  ( $n = 1, 2, 3$ ), and  $X$  is a light meson. Currently, the  $1P$  states  $D_0^*(2400)^0$  and  $D_0^*(2400)^+$  have been well studied, while  $2P$  and  $3P$  states haven't. The newly detected  $D_J^*(3000)^{+,0}$  are treated as the  $2P$  scalars in this paper and our results will help to determine their quantum numbers. The processes of  $B$  leptonic decays to them could be their important production ways.

In our previous study [27], we found that large relativistic corrections exist in the processes where a heavy-light excited state is involved. We also found that the highly excited state has larger relativistic effect than its corresponding ground state. Thus when a process includes

an excited state, a relativistic method or model is needed. In this paper, we use the Bethe-Salper (BS) method based on the relativistic BS equation. The relativistic effect is well concerned by solving the BS equation and applying the BS wave function.

The rest contents of this paper are organized as follows: in section 2, we present the formalism of semi-leptonic production process, including the leptonic and hadronic matrix elements by using the BS method. Then the factorization approach is used to derive the formalism of non-leptonic process in section 3. In section 4, we show our numerical results and comparison with the results of other model. Finally, discussions and short summary are given in section 4.

## II. FORMALISM OF SEMI-LEPTONIC DECAYS

We take  $B^-(\bar{B}^0) \rightarrow D_0^{*0}(D_0^{*+})\ell^-\bar{\nu}_\ell$  as an example to show the calculation details of semi-leptonic process. The Feynman diagram is shows in Fig. 1.

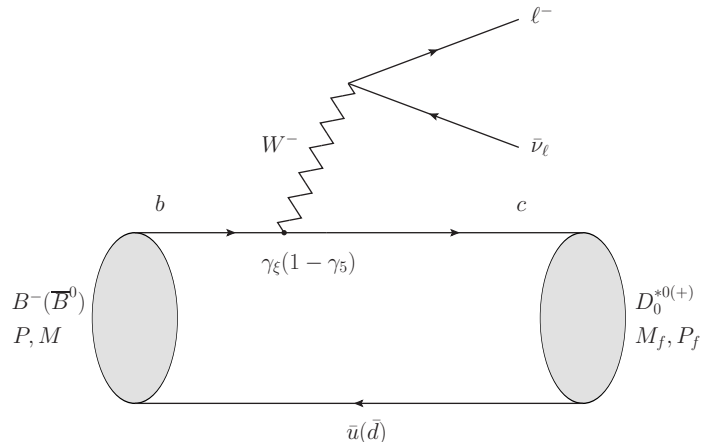


FIG. 1. Feynman diagram of the semi-leptonic decay  $B^-(\bar{B}^0) \rightarrow D_0^{*0(+)}\ell^-\bar{\nu}_\ell$ .

The transition amplitude  $T$  can be expressed as :

$$T = \frac{G_F}{\sqrt{2}} V_{cb} l^\xi \langle D_0^*(P_f) | J_\xi | B^-(P) \rangle, \quad (1)$$

where  $G_F$  is the Fermi weak coupling constant,  $V_{cb}$  is the CKM matrix element,  $J_\xi$  is the charged weak current and  $l^\xi$  is the leptonic matrix.

$$J_\xi = \bar{c}\gamma_\xi(1 - \gamma_5)b, \quad (2)$$

$$l^\xi = \bar{u}_\ell(p_l)\gamma^\xi(1 - \gamma_5)v_\nu(p_\nu). \quad (3)$$

Then the square of amplitude can be expressed by the function of hadronic and leptonic tensor,

$$|T|^2 = \frac{G_F^2}{2} |V_{cb}|^2 l^{\xi\xi'} h_{\xi\xi'}, \quad (4)$$

where the leptonic tensor can be written as following form:

$$l^{\xi\xi'} = 8(p_\nu^\xi p_\ell^{\xi'} + p_\ell^\xi p_\nu^{\xi'} - p_\ell \cdot p_\nu g^{\xi\xi'} + i\varepsilon^{\xi\xi'p_\ell p_\nu}). \quad (5)$$

We derive the hadronic matrix element by using the relativistic BS method

$$\begin{aligned} h_\xi &= \langle D_0^*(P_f) | J_\xi | B^-(P) \rangle \\ &= \int \frac{d^3q}{(2\pi)^3} \text{Tr} \left[ \frac{\not{P}}{M} \bar{\varphi}_{P_f}(q_{f\perp}) \gamma_\xi (1 - \gamma_5) \varphi_P(q_\perp) \right] = n_1 P_\xi + n_2 P_{f\xi}, \end{aligned} \quad (6)$$

where  $q_f = q - \frac{m_u}{m_b + m_u} P_f$ ,  $\varphi_P$  and  $\varphi_{P_f}$  are the instantaneous BS wave functions of the initial state  $B$  meson and final state  $D_0^*$  mesons. They are obtained by completely solving the BS equation. The processes of solving the Salpeter equation and obtaining the wave functions are not shown here. More details can be found in our previous works [28–30]. We just give a brief review in the appendix.  $n_i$  are the form factors whose results are shown in next section.

$h_{\xi\xi'}$  is the hadronic tensor,

$$\begin{aligned} h_{\xi\xi'} &= \langle D_0^*(P_f) | J_\xi | B^-(P) \rangle^\dagger \langle D_0^*(P_f) | J_{\xi'} | B^-(P) \rangle \\ &= n_1^2 P_\xi P_{\xi'} + n_2^2 P_{f\xi} P_{f\xi'} + n_1 n_2 (P_\xi P_{f\xi'} + P_{f\xi} P_{\xi'}). \end{aligned} \quad (7)$$

Then the decay width can be given by the phase-space integral

$$\Gamma = \frac{1}{2M} \int \frac{d^3\mathbf{P}_f d^3\mathbf{p}_\ell d^3\mathbf{p}_{\nu_\ell}}{(2\pi)^9 2E_f 2E_\ell 2E_{\nu_\ell}} (2\pi)^4 \delta^4(P - P_f - p_\ell - p_{\nu_\ell}) |T|^2. \quad (8)$$

After the simplification, it can be rewritten as

$$\Gamma = \frac{1}{64\pi M} \int |T|^2 \frac{|\mathbf{P}_f|}{E_f} d|\mathbf{P}_f| \frac{|\mathbf{p}_\ell|}{E_\ell} d|\mathbf{p}_\ell|. \quad (9)$$

### III. FORMALISM OF NON-LEPTONIC DECAYS

The Feynman diagram of non-leptonic decay  $B^- \rightarrow D_0^{*0} X$  or  $\bar{B}^0 \rightarrow D_0^{*+} X$  is shown in Fig. 2, where  $X$  could be  $\pi^-$ ,  $K^-$ ,  $\rho^-$  or  $K^{*-}$ .

The effective Hamiltonian  $\mathcal{H}_{eff}$  can be expressed as [31, 32]:

$$\mathcal{H}_{eff} = \frac{G_F}{2} [V_{cb} V_{uq}^* (c_1(\mu) O_1 + c_2(\mu) O_2) + h.c.], \quad (10)$$

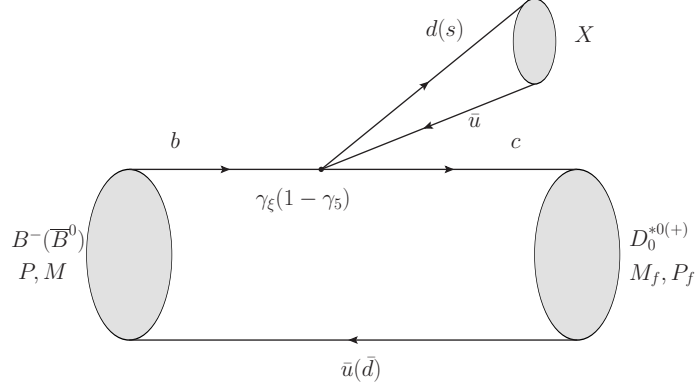


FIG. 2. Feynman diagram of the non-leptonic decay  $B^-(\bar{B}^0) \rightarrow D_0^{*0(+)} X$ .

where,  $O_i$  is the 4-quark operator containing the charged weak current  $(\bar{q}u)_{V-A}$  and  $(\bar{c}b)_{V-A}$ ;  $c_i$  is the Wilson coefficient which depends on the renormalization scale  $\mu$ .

By using the factorization approach, the transition matrix elements  $\langle D_0^* X | \mathcal{H}_{eff} | B \rangle$  involving the 4-quark operators can be split into the product of two matrix elements  $\langle D_0^* | (\bar{c}b)_{V-A} | B \rangle$  and  $\langle X | (\bar{q}u)_{V-A} | 0 \rangle$  [31, 33, 34].

Then the transition amplitude can be expressed as

$$T = \frac{G_F}{\sqrt{2}} V_{cb} V_{uq}^* a_1(\mu) \langle D_0^{*0} | (\bar{c}b)_{V-A} | B^- \rangle \langle X | (\bar{q}u)_{V-A} | 0 \rangle, \quad (11)$$

where,  $q$  denotes the  $d$  or  $s$  quark;  $a_1 = c_1 + \frac{1}{N_c} c_2$  is the effective Wilson coefficient, where  $N_c = 3$  is the number of colors. We choose the scale  $\mu \approx m_b$  for  $B$  decays and adopt the effective Wilson coefficient  $a_1 = 1.14$  [35]. The annihilation matrix element can be written as

$$\begin{aligned} \langle X_P | (\bar{q}u)_{V-A}^\mu | 0 \rangle &= -i f_X P_X^\mu, \\ \langle X_V | (\bar{q}u)_{V-A}^\mu | 0 \rangle &= f_X M_X \varepsilon_X^\mu, \end{aligned} \quad (12)$$

where  $X_P$  means pseudoscalar ( $\pi, K$ ) and  $X_V$  means vector mesons ( $\rho, K^*$ );  $f_X$  is the corresponding decay constant;  $\varepsilon^\mu$  is the polarization vector of  $X_V$  and it satisfies the completeness relation  $\sum \varepsilon_\lambda^\mu \varepsilon_\lambda^\nu = \frac{P_X^\mu P_X^\nu}{M_X^2} - g^{\mu\nu}$ .

Same as the semi-leptonic case, we write the square of amplitude by the hadronic and light meson tensor

$$|T|^2 = \frac{G_F^2}{2} |V_{ub}|^2 |V_{uq}|^2 a_1^2 h_{\mu\nu} X^{\mu\nu}, \quad (13)$$

where  $h_{\mu\nu}$  is same as Eq. 7, and the light meson tensor is

$$\begin{aligned} X_P^{\mu\nu} &= P_X^\mu P_X^\nu f_X^2, \\ X_V^{\mu\nu} &= (P_X^\mu P_X^\nu - M_X^2 g^{\mu\nu}) f_X^2. \end{aligned} \tag{14}$$

Then the decay width can be obtained by

$$\Gamma = \int \frac{|\mathbf{P}_f|}{32\pi^2 M^2} \sum |T|^2 d\Omega. \tag{15}$$

#### IV. RESULTS AND DISCUSSION

In our calculations, we adopt the same parameters as what we used before[26]:  $m_u = 0.305$  GeV,  $m_d = 0.311$  GeV,  $m_s = 0.50$  GeV,  $m_c = 1.62$  GeV,  $\alpha = 0.060$  GeV,  $\lambda = 0.210$  GeV<sup>2</sup> and  $\Lambda_{QCD} = 0.270$  GeV. The involved mesons' masses are:  $M_{D_0^*(2400)^0} = 2.318$  GeV,  $M_{D_0^*(2400)^+} = 2.351$  GeV,  $M_{D_0^*(3000)^{(0,+)} } = 3.008$  GeV,  $M_{D_0^*(3P)^{0,+}} = 3.183$  GeV,  $M_{B^0} = 5.2796$  GeV and  $M_{B^\pm} = 5.2793$  GeV.

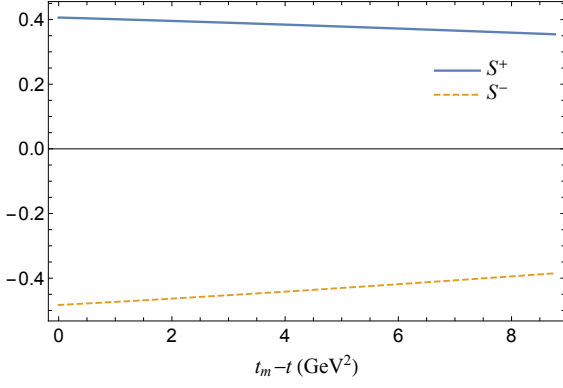
The CKM matrix elements[36] and the involved mesons' decay constants are[19, 36, 37]:  $|V_{cb}| = 0.0422$ ,  $|V_{ud}| = 0.9742$ ,  $|V_{us}| = 0.2243$ ,  $f_\rho = 205$  MeV,  $f_\pi = 130.4$  MeV,  $f_\eta = 130$  MeV and  $f_k = 156.2$  MeV.

##### A. Semi-leptonic decays

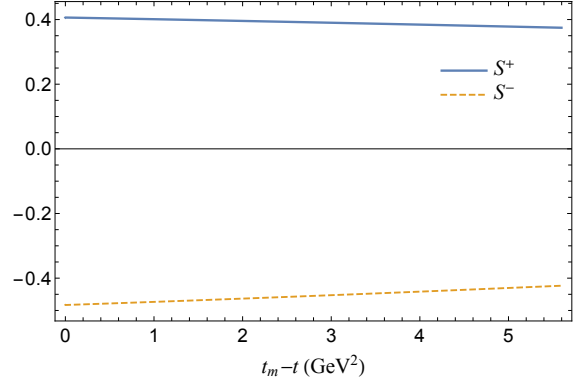
The form factors relevant to the hadronic transition matrix elements of  $B \rightarrow D_0^*(1P - 3P)\ell\nu_\ell$  are shown in Fig. 3, where  $t = (P - P_f)^2$  and  $t_m$  is the momentum transfer at the zero recoil(the maximum value of  $t$ ).

Table I shows the decay widths and branching ratios of semi-leptonic production of the ground state  $D_0^*(2400)$ . With varying the parameters by  $\pm 5\%$ , we can obtain the uncertainty of the results. Because there is almost no difference between the results of  $l = e$  and  $l = \mu$ , only the values of  $l = e$  are given below.

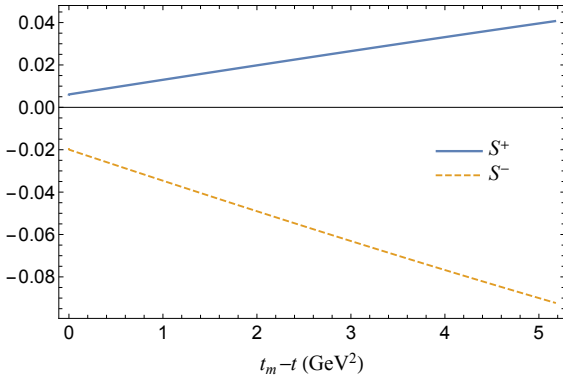
For comparison, we also give the results of cascade decays to  $D\pi$  which are shown in Table II. Recently, Ref.[16] used covariant light-front quark model to calculate the channel  $B^+ \rightarrow D_0^*(2400)^0 l^+ \bar{\nu}_l \rightarrow D^- \pi^+$ , whose result of branching ratio is  $2.31 \pm 0.25 \times 10^{-3}$ . And Ref.[17] shows that  $\mathcal{B}(B^+ \rightarrow \bar{D}_0^{*0} l^+ \nu_l) \times \mathcal{B}(\bar{D}_0^{*0} \rightarrow D^- \pi^+) = 2.15 \times 10^{-3}$  and  $\mathcal{B}(B^0 \rightarrow D_0^{*-} l^+ \nu_l) \times \mathcal{B}(D_0^{*-} \rightarrow D^0 \pi^-) = 1.80 \times 10^{-3}$  with the constituent quark model. Considering the uncertainty, our results are consistent with the experimental and other models' results.



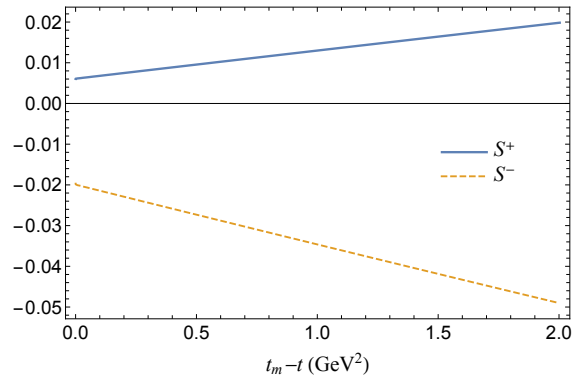
(a)The form factors for  $D_0^*(2400)$ ,  $l = e$  or  $\mu$



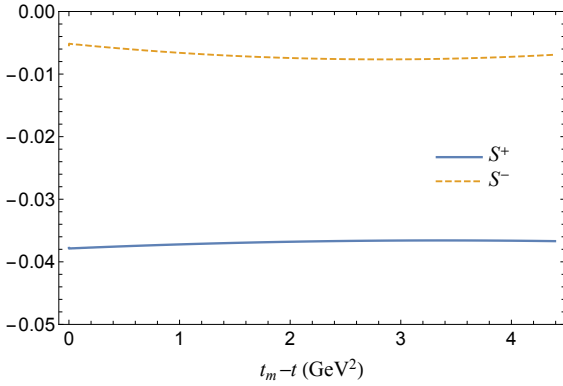
(b)The form factors for  $D_0^*(2400)$ ,  $l = \tau$



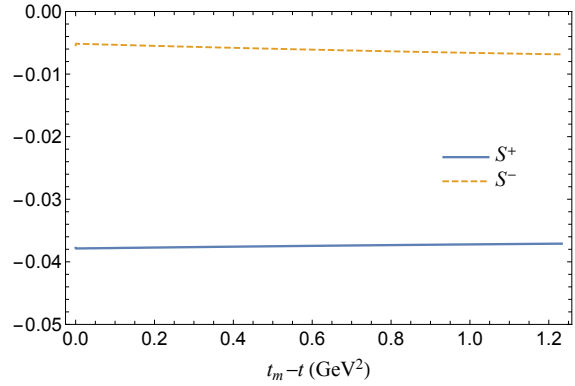
(c)The form factors for  $D_J^*(3000)$ ,  $l = e$  or  $\mu$



(d)The form factors for  $D_J^*(3000)$ ,  $l = \tau$



(e)The form factors for  $D_0^*(3P)$ ,  $l = e$  or  $\mu$



(f)The form factors for  $D_0^*(3P)$ ,  $l = \tau$

FIG. 3. The form factors for the semi-leptonic production process of  $D_0^*(2400)$ ,  $D_J^*(3000)$  and  $D_0^*(3P)$ , where  $S^+ = (n_1 + n_2)/2$ ,  $S^- = (n_1 - n_2)/2$ .

Then we use the same method to calculate the  $2P$  state  $D_J(3000)$ , which is shown in Table III. Unlike the ground state, the results of  $2P$  state are much lower and have large uncertainty by varying the input parameters, while the predicted results of  $3P$  state are

TABLE I. The results of semi-leptonic production of  $1P$  state  $D_0^*(2400)$

Channels	Widths (GeV)	BR
$B^- \rightarrow D_0^*(2400)^0 e^- \bar{\nu}_e$	$1.03 \sim 1.70 \times 10^{-15}$	$2.57 \sim 4.24 \times 10^{-3}$
$\bar{B}^0 \rightarrow D_0^*(2400)^+ e^- \bar{\nu}_e$	$1.04 \sim 1.69 \times 10^{-15}$	$2.39 \sim 3.91 \times 10^{-3}$
$B^- \rightarrow D_0^*(2400)^0 \tau^- \bar{\nu}_\tau$	$1.20 \sim 1.72 \times 10^{-16}$	$2.98 \sim 4.28 \times 10^{-4}$
$\bar{B}^0 \rightarrow D_0^*(2400)^+ \tau^- \bar{\nu}_\tau$	$1.13 \sim 1.60 \times 10^{-16}$	$2.62 \sim 3.70 \times 10^{-4}$

TABLE II. The branching ratios( $\times 10^{-3}$ ) of cascade decays to  $D\pi$ (with  $l = e$ ). The branching ratio  $\mathcal{B}(D_0^*(2400) \rightarrow D\pi)$  is from our previous work[26].

Channels	Ours	BABAR[9]	Belle[10]	PDG[36]
$\mathcal{B}(B^- \rightarrow D_0^*(2400)^0 e^- \bar{\nu}_l \rightarrow D^0 \pi^0)$	$0.85 \sim 1.39$			
$\mathcal{B}(B^- \rightarrow D_0^*(2400)^0 e^- \bar{\nu}_l \rightarrow D^+ \pi^-)$	$1.72 \sim 2.81$	$2.6 \pm 0.9$	$2.4 \pm 1.0$	$2.5 \pm 0.5$
$\mathcal{B}(\bar{B}^0 \rightarrow D_0^*(2400)^+ e^- \bar{\nu}_l \rightarrow D^0 \pi^+)$	$1.60 \sim 2.61$	$4.4 \pm 1.4$	$2.0 \pm 1.2$	$3.0 \pm 1.2$
$\mathcal{B}(\bar{B}^0 \rightarrow D_0^*(2400)^+ e^- \bar{\nu}_l \rightarrow D^+ \pi^0)$	$0.79 \sim 1.29$			

given in Table IV and get smaller uncertainty.

TABLE III. The results of semi-leptonic production of  $2P$  state  $D_J^*(3000)$

Channels	Widths (GeV)	BR
$B^- \rightarrow D_J^*(3000)^0 e^- \bar{\nu}_e$	$1.6 \sim 80.2 \times 10^{-18}$	$0.4 \sim 20.0 \times 10^{-5}$
$\bar{B}^0 \rightarrow D_J^*(3000)^+ e^- \bar{\nu}_e$	$1.2 \sim 83.0 \times 10^{-18}$	$0.3 \sim 19.2 \times 10^{-5}$
$B^- \rightarrow D_J^*(3000)^0 \tau^- \bar{\nu}_\tau$	$0.4 \sim 69.8 \times 10^{-20}$	$0.1 \sim 17.3 \times 10^{-7}$
$\bar{B}^0 \rightarrow D_J^*(3000)^+ \tau^- \bar{\nu}_\tau$	$0.8 \sim 72.9 \times 10^{-20}$	$0.2 \sim 16.8 \times 10^{-7}$

Why the same parameters varying leads to the abnormal results of excited states? We consider that the different structures of BS wave function possibly play an important role here. Fig. 4 shows the wave function values changing with the relative momentum $|q|$ . The wave functions of  $B^-$  and  $1P$  state are all positive without nodes. When we varying the input parameters, the curve will have some small shift. And the shift could cause the small uncertainty in the overlapping integral. For excited states, we can find that the wave functions have nodes. For  $2P$  states, the wave function changes from positive to negative after the nodes. In the overlapping integral, it causes the cancellation and the final results



TABLE IV. The results of semi-leptonic production of  $3P$  state  $D_0^*$

Channels	Widths (GeV)	BR
$B^- \rightarrow D_0^*(3P)^0 e^- \bar{\nu}_e$	$3.10 \sim 7.37 \times 10^{-18}$	$0.77 \sim 1.83 \times 10^{-5}$
$\bar{B}^0 \rightarrow D_0^*(3P)^+ e^- \bar{\nu}_e$	$3.24 \sim 7.88 \times 10^{-18}$	$0.75 \sim 1.82 \times 10^{-5}$
$B^- \rightarrow D_0^*(3P)^0 \tau^- \bar{\nu}_\tau$	$2.49 \sim 3.67 \times 10^{-20}$	$6.19 \sim 9.13 \times 10^{-8}$
$\bar{B}^0 \rightarrow D_0^*(3P)^+ \tau^- \bar{\nu}_\tau$	$2.45 \sim 3.78 \times 10^{-20}$	$5.65 \sim 8.73 \times 10^{-8}$

will be highly suppressed. Then if we vary the input parameters, a small shift of the wave function could cause a large uncertainty.

For  $3P$  states, the wave function has two nodes, and the value change from negative to positive after the second node. The cancellation gets smaller than the case of the  $2P$  state. Thus, the final branching ratio seems to be fine and the uncertainty is not very large.

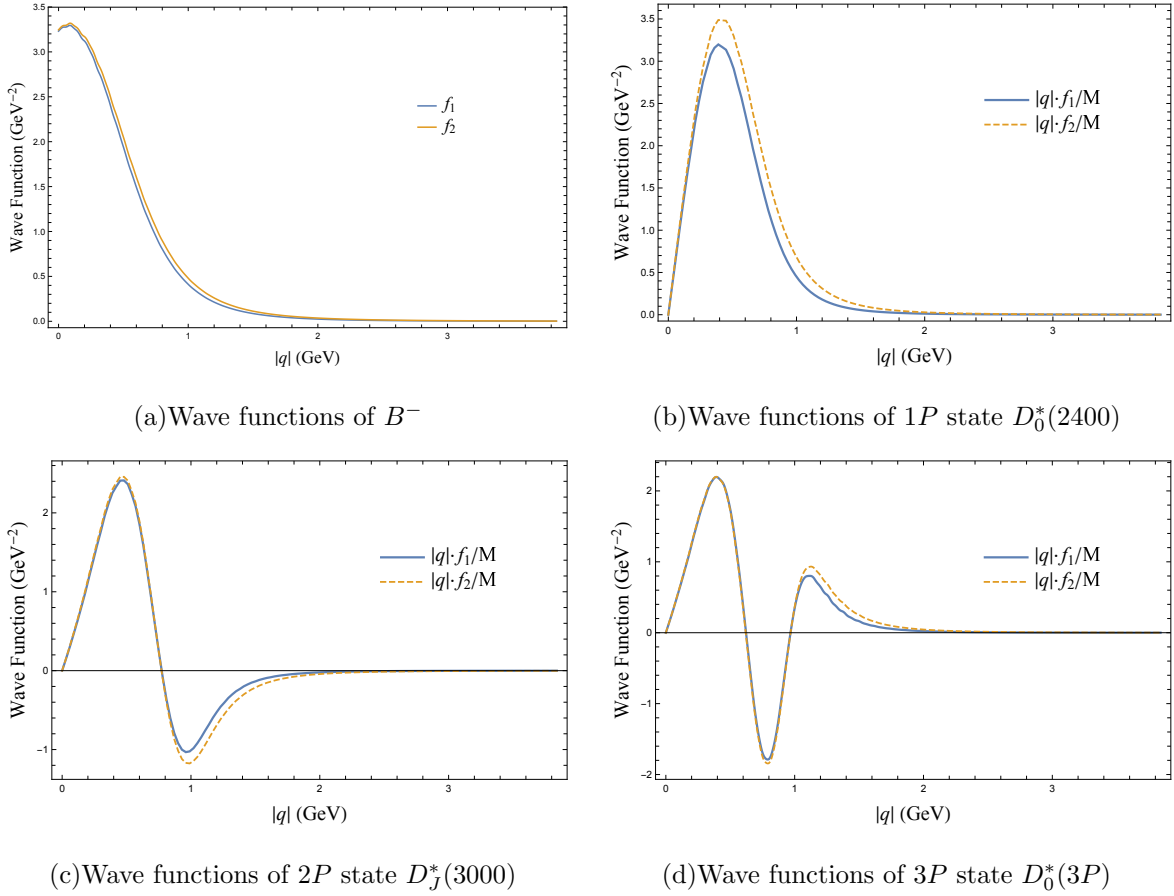


FIG. 4. Wave functions of  $B^-$  and  $D_0^*$ .

Considering the masses of these states have errors, the branching ratio of their semi-

leptonic production changing with their masses are given in Fig. 5. For  $1P$  state  $D_0^*(2400)$ , the results have small changes. But the branching ratio of  $2P$  state  $D_J^*(3000)$  dramatically decrease to nearly zero with increase of mass. The mass changing will also cause the wave function shift. That means the overlapping integral cancellation will increase as the mass increasing. For  $3P$  state, it can be seen that the curves of  $l = e$  have minimum points around  $m = 3.175$  GeV, which means the overlapping integrals have the maximum cancellation at that mass value. After that, the values increase again. For  $l = \tau$ , because of the small phase space, the branching ratios have the downtrend from the beginning to the end.

Then, the normalized lepton spectra of the semi-leptonic production are presented in Fig. 6. Because there are almost no difference between  $l = e$  and  $l = \mu$ , only the channels of  $B^- \rightarrow D_0^{*0} e^- \bar{\nu}_e$  and  $B^- \rightarrow D_0^{*0} \tau^- \bar{\nu}_\tau$  are given here. The spectrum peaks of  $2P$  and  $3P$  states move left because phase space decreases, especially for  $l = \tau$ .

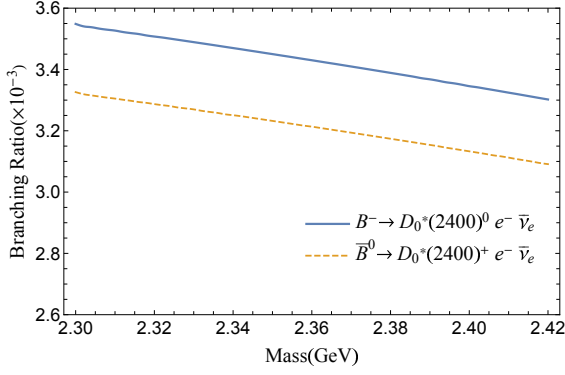
## B. Non-leptonic production

The non-leptonic production results of  $1P$  state  $D_0^*(2400)$  are shown in Table V. The  $D_0^* \pi$  and  $D_0^* \rho$  channels get the order of  $10^{-3}$ , while  $D_0^* K$  and  $D_0^* K^*$  modes are in the order of  $10^{-5}$  and  $10^{-4}$ , respectively.

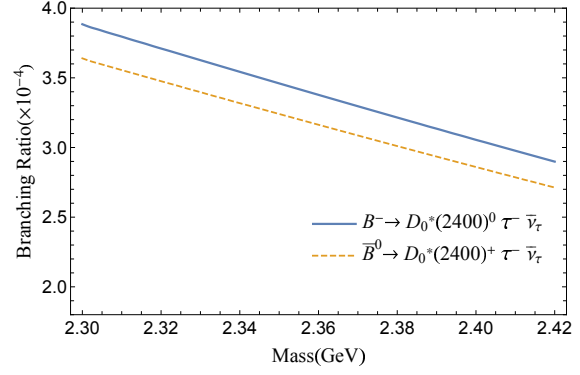
TABLE V. Non-leptonic production results of the  $1P$  state  $D_0^*(2400)$ .

Channels	Widths (GeV)	BR
$B^- \rightarrow D_0^*(2400)^0 \pi^-$	$3.35 \sim 5.78 \times 10^{-16}$	$0.83 \sim 1.44 \times 10^{-3}$
$\bar{B}^0 \rightarrow D_0^*(2400)^+ \pi^-$	$3.46 \sim 5.80 \times 10^{-16}$	$0.80 \sim 1.34 \times 10^{-3}$
$B^- \rightarrow D_0^*(2400)^0 K^-$	$2.48 \sim 4.26 \times 10^{-17}$	$0.62 \sim 1.06 \times 10^{-5}$
$\bar{B}^0 \rightarrow D_0^*(2400)^+ K^-$	$2.56 \sim 4.27 \times 10^{-17}$	$5.91 \sim 9.85 \times 10^{-6}$
$B^- \rightarrow D_0^*(2400)^0 \rho^-$	$0.74 \sim 1.30 \times 10^{-15}$	$1.85 \sim 3.23 \times 10^{-3}$
$\bar{B}^0 \rightarrow D_0^*(2400)^+ \rho^-$	$0.76 \sim 1.30 \times 10^{-15}$	$1.77 \sim 2.99 \times 10^{-3}$
$B^- \rightarrow D_0^*(2400)^0 K^{*-}$	$4.25 \sim 7.46 \times 10^{-17}$	$1.06 \sim 1.86 \times 10^{-4}$
$\bar{B}^0 \rightarrow D_0^*(2400)^+ K^{*-}$	$4.37 \sim 7.44 \times 10^{-17}$	$1.01 \sim 1.72 \times 10^{-4}$

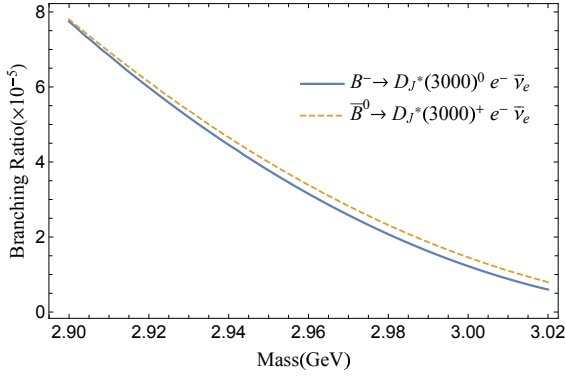
There have been some experimental results of their cascade decays. For comparison, our results of the cascade decays are shown in Table VI. The Belle and BABAR Collaborations show that the branching ratios  $\mathcal{B}(B^- \rightarrow D_0^{*0} \pi^-) \times \mathcal{B}(D_0^{*0} \rightarrow D^+ \pi^-)$  are  $(6.1 \pm 0.6 \pm 0.9 \pm$



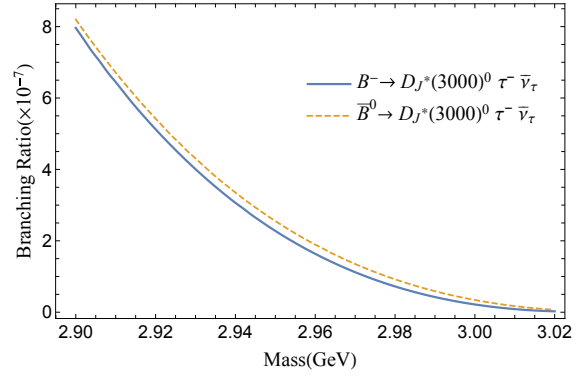
(a) Branching ratio vers the mass of  $D_0^*(2400), l = e$



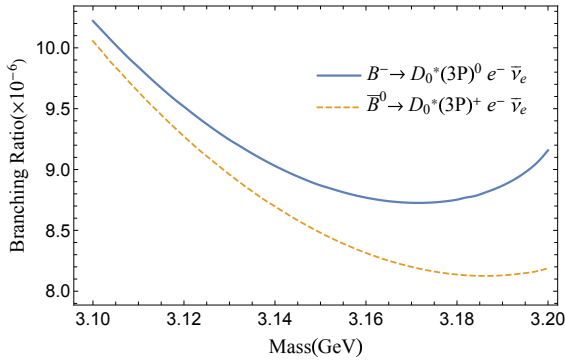
(b) Branching ratio vers the mass of  $D_0^*(2400), l = \tau$



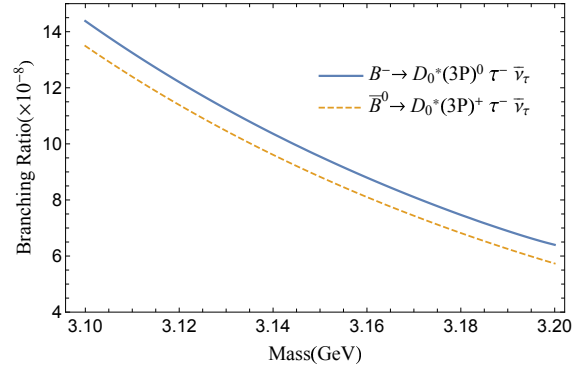
(c) Branching ratio vers the mass of  $D_J^*(3000), l = e$



(d) Branching ratio vers the mass of  $D_J^*(3000), l = \tau$



(e) Branching ratio vers the mass of  $D_J^*(3P), l = e$



(f) Branching ratio vers the mass of  $D_J^*(3P), l = \tau$

FIG. 5. The branching ratios of semi-leptonic production change with the mass of  $D_0^*$ .

$1.6) \times 10^{-4}$ [11] and  $(6.8 \pm 0.3 \pm 0.4 \pm 2.0) \times 10^{-4}$ [13], respectively. Our results are consistent with them. For the charged  $D_0^{*\pm}$  meson, the Belle and LHCb Collaborations give the results  $\mathcal{B}(\bar{B}^0 \rightarrow D_0^{*+} \pi^-) \times \mathcal{B}(D_0^{*+} \rightarrow D^0 \pi^+) = (6.0 \pm 1.3 \pm 1.5 \pm 2.2) \times 10^{-5}$ [12] and

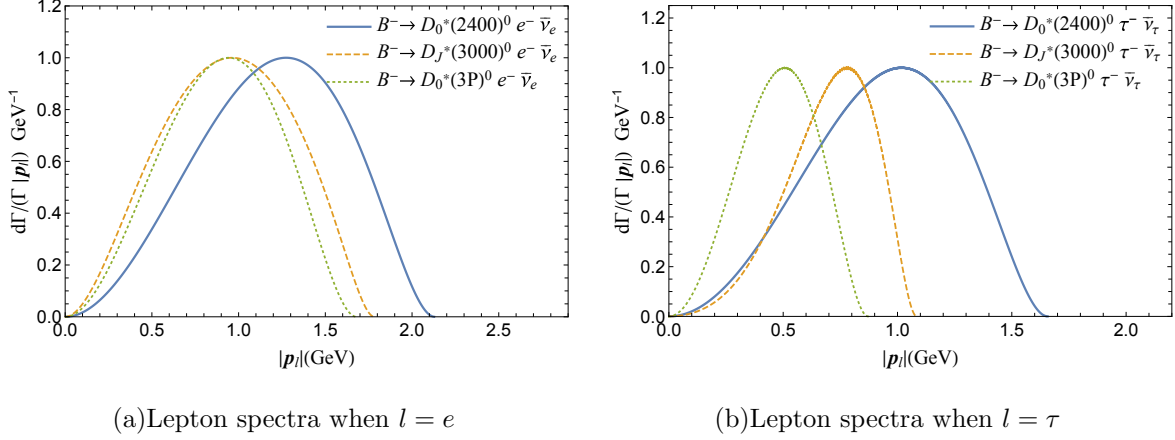


FIG. 6. The spectra of differential decay width vs  $|\mathbf{p}_l|$ (with normalization).

$(7.7 \pm 0.5 \pm 0.3 \pm 0.3 \pm 0.4) \times 10^{-5}$ [14], respectively, which are much lower than the branching ratio of the previous channel. For  $D_0^* K$  channel, the LHCb collaboration shows the result  $\mathcal{B}(B^- \rightarrow D_0^{*0} K^-) \times \mathcal{B}(D_0^{*0} \rightarrow D^+ \pi^-) = (6.1 \pm 1.9 \pm 0.5 \pm 1.4 \pm 0.4) \times 10^{-6}$ [38], which is also lower than our calculation. From the perspective of symmetry, the non-leptonic results of these channels should be similar. But different experimental results show marked discrepancy, which need more experimental data accumulations and theoretical attentions.

TABLE VI. The branching ratios of cascade decays to  $D\pi$ .

Channels	BR	Channels	BR
$B^- \rightarrow D_0^*(2400)^0 \pi^-$	$\rightarrow D^0 \pi^0$ $2.76 \sim 4.76 \times 10^{-4}$	$\bar{B}^0 \rightarrow D_0^*(2400)^+ \pi^-$	$\rightarrow D^0 \pi^+$ $5.34 \sim 8.94 \times 10^{-4}$
	$\rightarrow D^+ \pi^-$ $5.57 \sim 9.63 \times 10^{-4}$		$\rightarrow D^+ \pi^0$ $2.66 \sim 4.45 \times 10^{-4}$
$B^- \rightarrow D_0^*(2400)^0 K^-$	$\rightarrow D^0 \pi^0$ $2.04 \sim 3.51 \times 10^{-5}$	$\bar{B}^0 \rightarrow D_0^*(2400)^+ K^-$	$\rightarrow D^0 \pi^+$ $3.95 \sim 6.58 \times 10^{-5}$
	$\rightarrow D^+ \pi^-$ $4.12 \sim 7.09 \times 10^{-5}$		$\rightarrow D^+ \pi^0$ $1.96 \sim 3.27 \times 10^{-5}$
$B^- \rightarrow D_0^*(2400)^0 \rho^-$	$\rightarrow D^0 \pi^0$ $0.61 \sim 1.07 \times 10^{-3}$	$\bar{B}^0 \rightarrow D_0^*(2400)^+ \rho^-$	$\rightarrow D^0 \pi^+$ $1.18 \sim 2.00 \times 10^{-3}$
	$\rightarrow D^+ \pi^-$ $1.23 \sim 2.16 \times 10^{-3}$		$\rightarrow D^+ \pi^0$ $5.86 \sim 9.93 \times 10^{-4}$
$B^- \rightarrow D_0^*(2400)^0 K^{*-}$	$\rightarrow D^0 \pi^0$ $3.50 \sim 6.15 \times 10^{-5}$	$\bar{B}^0 \rightarrow D_0^*(2400)^+ K^{*-}$	$\rightarrow D^0 \pi^+$ $0.68 \sim 1.15 \times 10^{-4}$
	$\rightarrow D^+ \pi^-$ $0.71 \sim 1.24 \times 10^{-4}$		$\rightarrow D^+ \pi^0$ $3.35 \sim 5.71 \times 10^{-5}$

Then, like the previous section, the non-leptonic productions of  $2P$  and  $3P$  states are also considered and the results are shown in Table VII and VIII, respectively.

Similar to the semi-leptonic occasion, the results of  $2P$  state  $D_0^*(3000)$  have a large uncertainty, which can also be explained by the node structure of BS wave function. Because the phase spaces of  $2P$  and  $3P$  state are close, their branching ratios reach similar magnitude.

We also draw the branching ratios changing with the mass of  $D_0^*$  in Fig. 7. Like the semi-

TABLE VII. Non-leptonic production results of the  $2P$  state  $D_0^*(3000)$ .

Channels	Widths (GeV)	BR
$B^- \rightarrow D_0^*(3000)^0 \pi^-$	$0.07 \sim 54.7 \times 10^{-18}$	$0.02 \sim 13.4 \times 10^{-5}$
$\bar{B}^0 \rightarrow D_0^*(3000)^+ \pi^-$	$0.003 \sim 55.3 \times 10^{-18}$	$0.0006 \sim 12.8 \times 10^{-5}$
$B^- \rightarrow D_0^*(3000)^0 K^-$	$0.08 \sim 37.9 \times 10^{-19}$	$0.02 \sim 9.44 \times 10^{-6}$
$\bar{B}^0 \rightarrow D_0^*(3000)^+ K^-$	$0.02 \sim 39.0 \times 10^{-19}$	$0.004 \sim 9.02 \times 10^{-6}$
$B^- \rightarrow D_0^*(3000)^0 \rho^-$	$0.04 \sim 10.8 \times 10^{-17}$	$0.10 \sim 26.8 \times 10^{-5}$
$\bar{B}^0 \rightarrow D_0^*(3000)^+ \rho^-$	$0.01 \sim 11.1 \times 10^{-17}$	$0.03 \sim 25.7 \times 10^{-5}$
$B^- \rightarrow D_0^*(3000)^0 K^{*-}$	$0.28 \sim 59.0 \times 10^{-19}$	$0.07 \sim 14.7 \times 10^{-6}$
$\bar{B}^0 \rightarrow D_0^*(3000)^+ K^{*-}$	$0.11 \sim 61.2 \times 10^{-19}$	$0.03 \sim 14.1 \times 10^{-6}$

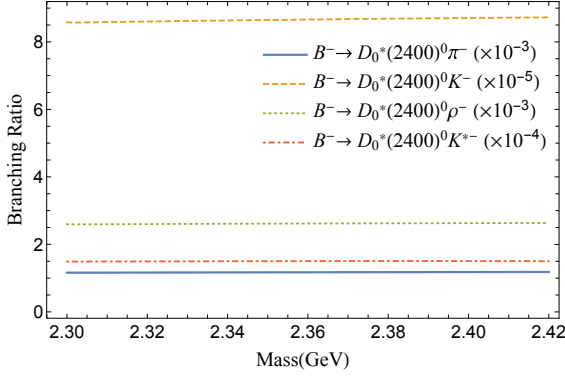
 TABLE VIII. Non-leptonic production results of the  $3P$  state  $D_0^*$ .

Channels	Widths (GeV)	BR
$B^- \rightarrow D_0^*(3P)^0 \pi^-$	$1.87 \sim 5.59 \times 10^{-18}$	$0.47 \sim 1.39 \times 10^{-5}$
$\bar{B}^0 \rightarrow D_0^*(3P)^+ \pi^-$	$1.86 \sim 6.00 \times 10^{-18}$	$0.43 \sim 1.39 \times 10^{-5}$
$B^- \rightarrow D_0^*(3P)^0 K^-$	$1.43 \sim 4.02 \times 10^{-19}$	$0.36 \sim 1.00 \times 10^{-6}$
$\bar{B}^0 \rightarrow D_0^*(3P)^+ K^-$	$1.41 \sim 4.30 \times 10^{-19}$	$0.33 \sim 0.99 \times 10^{-6}$
$B^- \rightarrow D_0^*(3P)^0 \rho^-$	$0.38 \sim 1.03 \times 10^{-17}$	$0.96 \sim 2.56 \times 10^{-5}$
$\bar{B}^0 \rightarrow D_0^*(3P)^+ \rho^-$	$0.38 \sim 1.11 \times 10^{-17}$	$0.89 \sim 2.55 \times 10^{-5}$
$B^- \rightarrow D_0^*(3P)^0 K^{*-}$	$2.10 \sim 5.47 \times 10^{-19}$	$0.52 \sim 1.36 \times 10^{-6}$
$\bar{B}^0 \rightarrow D_0^*(3P)^+ K^{*-}$	$2.11 \sim 5.89 \times 10^{-19}$	$0.49 \sim 1.36 \times 10^{-6}$

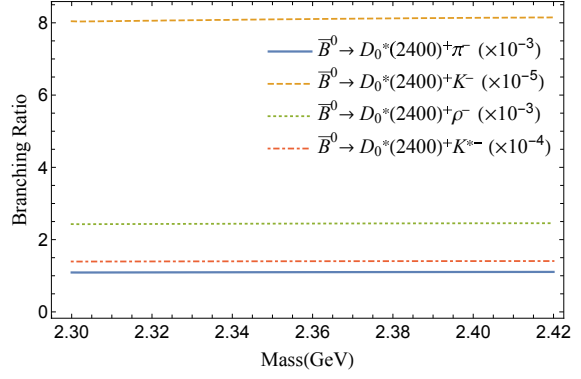
leptonic production case, the non-leptonic production results of  $2P$  state are sensitive to the mass. The curves of  $1P$  and  $3P$  states stay relatively stable when the mass values change. There are also minimum points of  $3P$  states' curves at 3.175 GeV, where the maximum cancellation of overlapping integral occurs.

## V. SUMMARY

Based on the instantaneous BS framework, we calculate the semi-leptonic and non-leptonic productions of several excited  $D_0^*$  states from  $B$  mesons. For  $1P$  state  $D_0^*(2400)$ ,

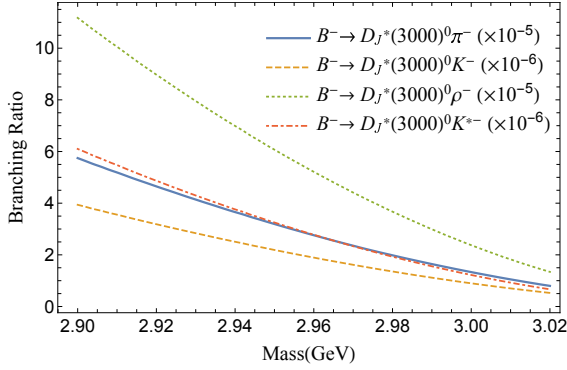


(a) Branching ratio vers the mass of  $1P$  state



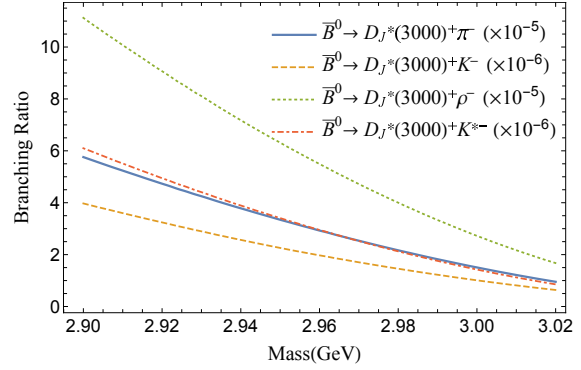
(b) Branching ratio vers the mass of  $1P$  state

$D_0^*(2400)^0$



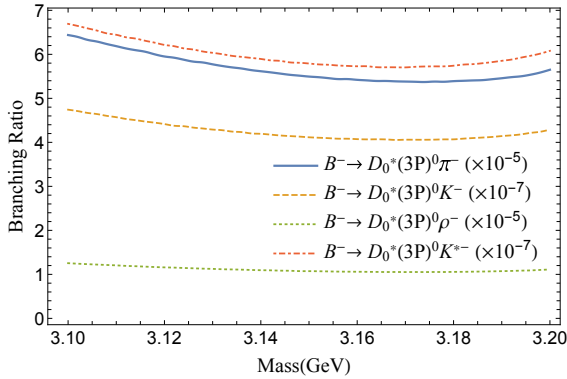
(c) Branching ratio vers the mass of  $2P$  state

$D_0^*(2400)^+$



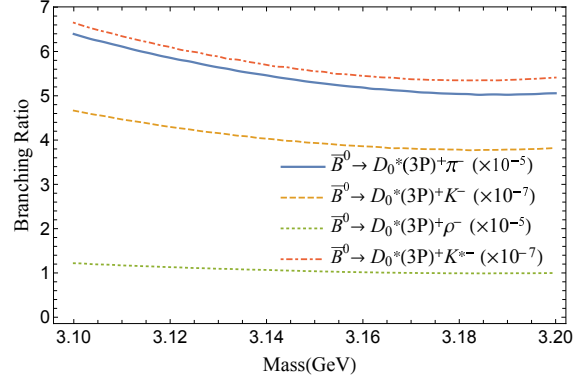
(d) Branching ratio vers the mass of  $2P$  state

$D_J^*(3000)^0$



(e) Branching ratio vers the mass of  $3P$  state

$D_J^*(3000)^+$



(f) Branching ratio vers the mass of  $3P$  state

$D_0^*(3183)^0$

$D_0^*(3183)^+$

FIG. 7. The branching ratios of non-leptonic production of  $D_0^*$ .

the branching ratios of  $B \rightarrow D_0^* e^- \bar{\nu}_e$  are in the order of  $10^{-3}$ , which is consistent with the results of present experiments and other models. For non-leptonic channels, the experiments

didn't get quite consistent results while our calculating consists with parts of present experimental results. For  $2P$  states  $D_J^*(3000)$ , we get suppressed branching ratios in the order of  $10^{-5} \sim 10^{-6}$  and large uncertainty in both semi-leptonic and non-leptonic channels. The cancellation in overlapping integral, which is caused by its one-nodes structure of the BS wave functions, could explain the abnormal results. For  $3P$  states, their ratios are of the same order of magnitude as  $2P$  states' results because they have similar phase spaces. The two-nodes structure of  $3P$  states wave functions makes the cancellation smaller than that of  $2P$  states and get the minimum branching ratios if their masses are around 3.175 GeV. Our work could give some inspiration to future experiment and we expect more attention on these production processes of the orbitally excited  $D$  mesons.

## ACKNOWLEDGEMENTS

This work was supported in part by the National Natural Science Foundation of China (NSFC) under Grant No. 11575048, No. 11405037, No. 11505039. We thank the HPC Studio at Physics Department of Harbin Institute of Technology for access to computing resources through INSPUR-HPC@PHY.HIT.

## APPENDIX BETHE-SALPETER WAVE FUNCTION

The general forms of wave functions are

$$\varphi_{0^+}(q_\perp) = M \left[ \frac{\not{q}_\perp}{M} f_{a1}(q_\perp) + \frac{\not{P}\not{q}_\perp}{M^2} f_{a2}(q_\perp) + f_{a3}(q_\perp) + \frac{\not{P}}{M} f_{a4}(q_\perp) \right], \quad (1)$$

$$\varphi_{0^-}(q_\perp) = M \left[ \frac{\not{P}}{M} f_{b1}(q_\perp) + f_{b2}(q_\perp) + \frac{\not{q}_\perp}{M} f_{b3}(q_\perp) + \frac{\not{P}\not{q}_\perp}{M^2} f_{b4}(q_\perp) \right] \gamma_5, \quad (2)$$

where the constraint conditions are

$$f_{a3} = \frac{q_\perp^2(\omega_1 + \omega_2)}{M(m_1\omega_2 + m_2\omega_1)} f_{a1}, \quad f_{a4} = \frac{q_\perp^2(\omega_1 - \omega_2)}{M(m_1\omega_2 + m_2\omega_1)} f_{a2}, \quad (3)$$

$$f_{b3} = \frac{M(\omega_2 - \omega_1)}{m_1\omega_2 + m_2\omega_1} f_{b2}, \quad f_{b4} = -\frac{M(\omega_1 + \omega_2)}{m_1\omega_2 + m_2\omega_1} f_{b1}. \quad (4)$$

The positive parts are expressed as

$$\varphi_{0^+}^{++}(q_\perp) = A_1 + A_2 \frac{\not{P}}{M} + A_3 \frac{\not{q}_\perp}{M} + A_4 \frac{\not{P}\not{q}_\perp}{M^2}, \quad (5)$$

$$\varphi_{0^-}^{++}(q_\perp) = \left[ B_1(q_\perp) + \frac{\not{P}}{M} B_2(q_\perp) + \frac{\not{P}}{M} B_3(q_\perp) + \frac{\not{P} \not{q}_\perp}{M^2} B_4(q_\perp) \right] \gamma_5, \quad (6)$$

where

$$A_1 = \frac{(\omega_1 + \omega_2)q_\perp^2}{2(m_1\omega_2 + m_2\omega_1)} \left( f_{a1} + \frac{m_1 + m_2}{\omega_1 + \omega_2} f_{a2} \right), \quad A_3 = \frac{M}{2} \left( f_{a1} + \frac{m_1 + m_2}{\omega_1 + \omega_2} f_{a2} \right), \quad (7)$$

$$A_2 = \frac{(m_1 - m_2)q_\perp^2}{2(m_1\omega_2 + m_2\omega_1)} \left( f_{a1} + \frac{m_1 + m_2}{\omega_1 + \omega_2} f_{a2} \right), \quad A_4 = \frac{M}{2} \left( \frac{\omega_1 + \omega_2}{m_1 + m_2} f_{a1} + f_{a2} \right),$$

$$B_1 = \frac{M}{2} \left( \frac{\omega_1 + \omega_2}{m_1 + m_2} f_{b1} + f_{b2} \right), \quad B_3 = -\frac{M(\omega_1 - \omega_2)}{m_1\omega_2 + m_2\omega_1} B_1, \quad (8)$$

$$B_2 = \frac{M}{2} \left( f_{b1} + \frac{m_1 + m_2}{\omega_1 + \omega_2} f_{b2} \right), \quad B_4 = -\frac{(m_1 + m_2)M}{m_1\omega_2 + m_2\omega_1} B_1.$$

- 
- [1] D. Buskulic et al. (ALEPH Collaboration), Physics Letters B **395**, 373 (1997).
  - [2] J. Bartelt et al. (CLEO Collaboration), Physical Review Letters **82**, 3746 (1999).
  - [3] G. Abbiendi et al. (OPAL Collaboration), Physics Letters B **482**, 15 (2000).
  - [4] K. Abe et al. (Belle Collaboration), Physics Letters B **526**, 258 (2002).
  - [5] B. Aubert et al. (BABAR Collaboration), Physical Review D **77**, 032002 (2008).
  - [6] B. Aubert et al. (BABAR Collaboration), Physical Review Letters **104**, 011802 (2010).
  - [7] W. Dungen, T. Aziz, et al. (Belle Collaboration), Physical Review D **82**, 112007 (2010).
  - [8] R. Glattauer, Schwanda, et al. (Belle Collaboration), Physical Review D **93**, 032006 (2016).
  - [9] B. Aubert et al. (The BABAR Collaboration), Phys. Rev. Lett. **101**, 261802 (2008).
  - [10] D. Liventsev et al. (The Belle Collaboration), Phys. Rev. D **77**, 091503 (2008).
  - [11] K. Abe et al. (Belle Collaboration), Phys. Rev. D **69**, 112002 (2004).
  - [12] A. Kuzmin et al. (Belle Collaboration), Phys. Rev. D **76**, 012006 (2007).
  - [13] B. Aubert, M. Bona, et al. (BABAR Collaboration), Physical Review D **79**, 112004 (2009), arXiv:0901.1291.
  - [14] R. Aaij et al. (LHCb Collaboration), Phys. Rev. D **92**, 032002 (2015).
  - [15] R. Aaij et al. (LHCb Collaboration), Phys. Rev. D **91**, 092002 (2015).
  - [16] X.-W. Kang, T. Luo, Y. Zhang, L.-Y. Dai, and C. Wang, The European Physical Journal C **78**, 909 (2018).
  - [17] J. Segovia, C. Albertus, D. R. Entem, F. Fernández, E. Hernández, and M. A. Pérez-García, Physical Review D **84**, 094029 (2011).



- [18] H.-F. Fu, G.-L. Wang, Z.-H. Wang, and X.-J. Chen, Chinese Physics Letters **28**, 121301 (2011).
- [19] R. Aaij et al. (LHCb Collaboration), JHEP **2013**, 145 (2013).
- [20] Y. Sun, X. Liu, and T. Matsuki, Phys. Rev. D **88**, 094020 (2013).
- [21] Q.-F. Lü and D.-M. Li, Phys. Rev. D **90**, 054024 (2014).
- [22] G.-L. Yu, Z.-G. Wang, Z.-Y. Li, and G.-Q. Meng, Chin. Phys. C **39**, 063101 (2015).
- [23] S. Godfrey and K. Moats, Phys. Rev. D **93**, 034035 (2016).
- [24] S.-C. Li, Y. Jiang, T.-H. Wang, Q. Li, Z.-H. Wang, and G.-L. Wang, Mod. Phys. Lett. A **32**, 1750013 (2017).
- [25] S.-C. Li, T. Wang, Y. Jiang, X.-Z. Tan, Q. Li, G.-L. Wang, and C.-H. Chang, Phys. Rev. D **97**, 054002 (2018).
- [26] X.-Z. Tan, T. Wang, Y. Jiang, S.-C. Li, Q. Li, G.-L. Wang, and C.-H. Chang, The European Physical Journal C **78**, 583 (2018).
- [27] Z.-K. Geng, T. Wang, Y. Jiang, G. Li, X.-Z. Tan, and G.-L. Wang, Phys. Rev. D **99**, 013006 (2019).
- [28] C. S. Kim and G.-L. Wang, Phys. Lett. **B584**, 285 (2004).
- [29] G.-L. Wang, Phys. Lett. B **633**, 492 (2006).
- [30] G.-L. Wang, Physics Letters B **650**, 15 (2007).
- [31] A. Ali, G. Kramer, and C.-D. Lü, Phys. Rev. D **58**, 094009 (1998).
- [32] H.-M. Choi and C.-R. Ji, Phys. Rev. D **80**, 114003 (2009).
- [33] D. Fakirov and B. Stech, Nuclear Physics B **133**, 315 (1978).
- [34] M. Bauer, B. Stech, and M. Wirbel, Zeitschrift für Physik C Particles and Fields **34**, 103 (1987).
- [35] M. A. Ivanov, J. G. Körner, and P. Santorelli, Physical Review D **73**, 054024 (2006).
- [36] M. Tanabashi et al. (Particle Data Group), Phys. Rev. D **98**, 030001 (2018).
- [37] Q. Li, Y. Jiang, T. Wang, H. Yuan, G.-L. Wang, and C.-H. Chang, Eur. Phys. J. C **77**, 297 (2017).
- [38] R. Aaij et al. (LHCb Collaboration), Phys. Rev. D **93**, 119901 (2016).